Demonstration of AlGaN-Delta-GaN QW by Plasma-Assisted Molecular Beam Epitaxy for 260 nm Ultraviolet Light Emitting Diodes

Cheng. Liu[1]*, Kevin Lee[2], S. M. Islam[2], Huili (Grace) Xing[2,3], Debdeep Jena[2,3], and Jing Zhang[1]**
[1]Department of Electrical and Microelectronic Engineering, Rochester Institute of Technology, Rochester, NY 14623, USA
[2]School of Electrical and Computer Engineering, and [3]Department of Materials Science and Engineering, Cornell University, Ithaca, NY 14850, USA

ABSTRACT

III-nitride ultraviolet (UV) light emitting diodes (LEDs) with emission wavelengths in the range of 250-280 nm have attracted considerable interest for applications such as germicidal disinfection and biological detection. However, the widely-used AlGaN quantum well (QW)-based LEDs at such wavelengths suffer from low quantum efficiencies. One main factor that limits the AlGaN QW LED efficiency at ~250-280 nm is the suffering of the severe band mixing effect caused by the valence subbands crossover, as well as the Quantum Confined Stark Effect (QCSE). Therefore, the novel AlGaN-delta-GaN QW design was proposed to address these issues in order to realize high-efficiency deep-UV LEDs.

Here, we proposed a novel $Al_{0.9}Ga_{0.1}N$-delta-GaN QW by inserting an ultra-thin delta-GaN layer into a conventional $Al_{0.9}Ga_{0.1}N$ QW active region. The physics from such QW design was investigated by 6-band $\boldsymbol{k \cdot p}$ model and the structure was experimentally demonstrated by Plasma-assisted Molecular Beam Epitaxy (PAMBE). The calculated results show that the insertion of delta-GaN layer could successfully address the band mixing issue and QCSE, leading to a significant improvement in spontaneous emission rate as compared to that of $Al_{0.55}Ga_{0.45}N$ QW at 260 nm. The 5-period $Al_{0.9}Ga_{0.1}N$-delta-GaN QW with 3-nm AlN barrier was grown on AlN/sapphire substrate by MBE with ~2-monolayer delta-GaN layer, which was evidenced by the cross-sectional transmission electron microscope. The two-photon photoluminescence spectrum presented a single peak emission centered at 260 nm from the grown $Al_{0.9}Ga_{0.1}N$-delta-GaN QW with a full width at half maximum of 12 nm, which shows that the demonstrated QW would be promising for high-efficiency UV LEDs.

Keywords: Ultraviolet, Plasma-Assisted MBE, Light-Emitting Diodes

INTRODUCTION

Ultraviolet (UV) light with emission wavelength of 200 nm - 300 nm is capable of inactivating microorganisms and proven to be a trustworthy disinfection method in drinking water purification[1-2]. Among all the UV emitters, UV light-emitting diodes (LEDs) are of great interest for this application because of their unique advantages, as compared to conventional low- and medium-pressure mercury lamps, such as compact and robust designs, high efficiency and long lifetime[1, 3-4]. Above all, the emitted wavelength from UV LEDs can be adjusted to the target regime by engineering the device designs. Recently, several research groups investigated the UV LEDs with emission wavelength of 260 nm[5-7], at which the UV light has maximum absorption rate through microorganisms' DNA[1-2]. However, the total external quantum efficiencies from such UV LEDs are still limited to ~10%[1, 8-9] due to the low carrier injection efficiency caused by the poor p-type doping in AlGaN alloy[1, 6, 10-11] and the low light extraction efficiency resulting from the light absorption and internal reflection[1, 7, 12]. In addition, the Quantum Confined Stark Effect (QCSE) in the widely used AlGaN quantum well (QW) is also a limiting factor for the low EQE in UV LEDs with emission wavelength of ~260 nm[13]. Specifically, the existence of the large polarization fields in III-nitride materials could shift the electron and hole

*cl7007@rit.edu; phone 1 585 298 6687

**Jing.Zhang@rit.edu

Gallium Nitride Materials and Devices XIII, edited by Jen-Inn Chyi, Hiroshi Fujioka,
Hadis Morkoç, Proc. of SPIE Vol. 10532, 105320W · © 2018 SPIE
CCC code: 0277-786X/18/$18 · doi: 10.1117/12.2290366

wave functions to opposite side of the QW and decrease the wave function overlap integral, which leads to reduced internal quantum efficiency[1, 13]. Therefore, some nanostructures that can significantly mitigate the QCSE in QW region needs to be developed for high efficiency deep-UV LED with emission wavelength of ~260 nm.

To address this issue, the use of delta-GaN QW design was proposed as a possible solution[14]. Specifically, an ultra-thin delta-GaN layer can be inserted into a 3-nm conventional AlGaN QW to form the AlGaN-delta-GaN QW. Based on simulation results, the authors realized that the insertion of the thin delta-GaN layer could not only flip the heavy hole (HH) subband back to the top of the valence band but also strongly localize electron and hole wave functions toward the QW center and improve the overlap integral in QW region. As a result, large spontaneous emission recombination rate was achieved theoretically by the use of AlGaN-delta-GaN QW for deep-UV LEDs. In addition, the emission wavelength from the proposed QW region can be adjusted by engineering the delta-GaN layer thickness and the Al-composition in QW region. Although promising results have been reported, the proposed AlGaN-delta-GaN QWs are still not demonstrated experimentally due to the difficulty in epitaxial growth. Recently, several research groups successfully grew ultrathin GaN layer for mid- and deep-UV emissions, such as AlN/GaN superlattices[15] and AlN/GaN QWs and quantum dots (QDs)[16-20], which enables epitaxial growth of the AlGaN-delta-GaN QW for deep-UV emissions.

Therefore, in this study, we designed an AlGaN-delta-GaN QW to realize the deep-UV emission at 260 nm. The Al-content and the delta-GaN layer thickness were selected to be 90% and 5 Å, respectively. The 6-band ***k·p*** model was employed in this study to simulate the band structure and the emission properties of the designed AlGaN-delta-GaN QW, which were compared to that of a conventional 3-nm AlGaN QW with Al-composition of 55%. The $Al_{0.9}Ga_{0.1}N$-delta-GaN QW was also grown in this study by plasma-assisted molecular beam epitaxy (PA-MBE) and characterized by reflection high-energy electron diffraction (RHEED), atomic force microscopy (AFM), X-ray diffraction (XRD), scanning transmission electron microscope (STEM) and two-photon photoluminescence (PL). Strong 260-nm emission is realized by both simulation and experiment, showing the AlGaN-delta-GaN QW could be a promising alternative for deep-UV LEDs.

CONCEPT AND PHYSICS OF ALGAN-DELTA-GAN QUANTUM WELL

The band structures and physics of the $Al_{0.9}Ga_{0.1}N$-delta-GaN QW are theoretically investigated by a 6 band ***k·p*** model in this work. The model takes into account the strain effect, polarization electric field and carrier screening effect. More simulation details and material parameters can be found from ref. 21. The band lineups and the ground state conduction band wave function(Ψ_{e1}) and the ground state heavy hole wave function (Ψ_{hh1}) of the $Al_{0.9}Ga_{0.1}N$-delta-GaN QW are plotted in figure 1 and compared to that of a conventional 3-nm AlGaN QW. The 55% Al-content in the conventional AlGaN QW was selected to achieve an emission wavelength of ~260 nm. As shown in figure 1(a), the electron and hole wave functions are largely separated due to the QCSE, which results in small wave function overlap integral of 14.47%. In contrast, the insertion of a 5-Å delta-GaN layer into the 3nm $Al_{0.9}Ga_{0.1}N$ QW provides a local minimum in the QW region and both wave functions are pushed toward the center of the QW. As a result, the overlap integral between the ground state conduction band and heavy hole band is boosted to be 84.58%. Note that the two $Al_{0.9}Ga_{0.1}N$ sub-QWs, together with the delta-GaN layer, forming the whole AlGaN-delta-GaN QW region. The significant enhancement of the electron and hole wave function overlap indicates the proposed $Al_{0.9}Ga_{0.1}N$-delta-GaN QW design suppresses the QCSE which is suffered in the conventional AlGaN QW, and large improvement in spontaneous emission recombination rate is expected.

The band-edge valence band structures for the $Al_{0.9}Ga_{0.1}N$-delta-GaN QW and 3-nm $Al_{0.55}Ga_{0.45}N$ QW are simulated and compared in this study. Previous publication mentioned the light polarization switches at an Al-composition of 68% in conventional 3-nm AlGaN QW[13]. For the AlGaN QW with an aluminum composition of 90%, crystal-field split-off (CH) subband occupies the highest energy level. The insertion of the delta-GaN layer into $Al_{0.9}Ga_{0.1}N$ QW could rearrange the heavy hole (HH) and light hole (LH) into higher energy levels, as shown in figure 2 (b). However, for the $Al_{0.55}Ga_{0.45}N$ QW, whose Al-composition is lower than the crossover point, HH subband is on the top of the valence band structure. Besides, the energy separations between HH/LH and CH subband for both $Al_{0.55}Ga_{0.45}N$ QW and $Al_{0.9}Ga_{0.1}N$-delta-GaN QW at Γ-point are relatively large, which enables most of the carriers populate at HH/LH subband. Figure 2 (c) and (d) plots all the transitions between the ground state conduction band to the four highest valence subbands for both structures. The matrix elements for the proposed AlGaN-delta-GaN QW are much larger than that of the conventional $Al_{0.55}Ga_{0.45}N$ QW, which is attributed to the significant improvement in the wave functions overlap. Note that although the ground state conduction band to CH subband transition (C-CH1) is larger than the ground state conduction band to heavy hole (C1-HH1) and light hole (C1-LH1) transitions for both structures, the large energy separation between HH/LH and CH subbands ensures the dominant C1-HH1 and C1-LH1, which indicates the transverse-electric (TE)-polarized emission is larger than transverse-magnetic (TM)-polarized emission for both QW structures.

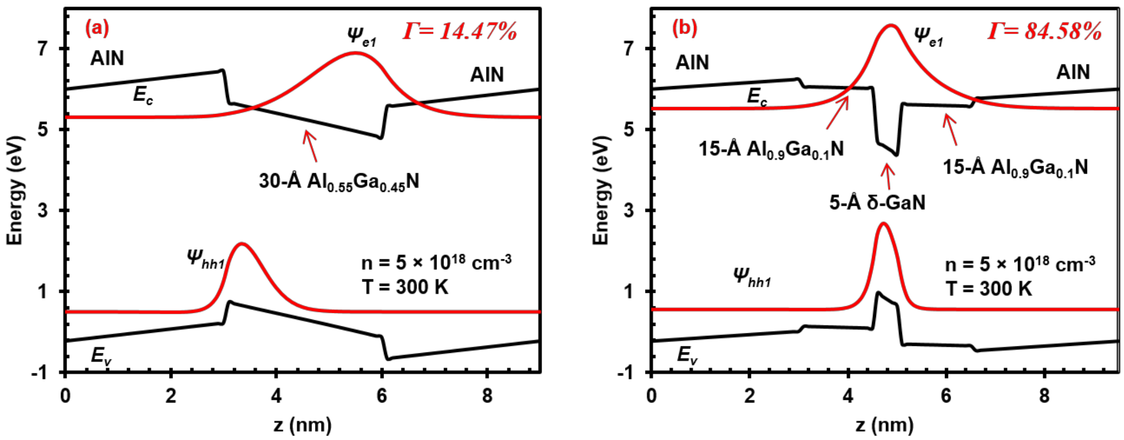

Figure 1. Energy band lineups with ground state electron wavefunction (ψ_{e1}) and heavy hole wavefunction (ψ_{hh1}) at room temperature for (a) $Al_{0.55}Ga_{0.45}N$ QW (b) $Al_{0.9}Ga_{0.1}N$-delta-GaN QW. The carrier density is $n = 5\times10^{18}$ cm^{-3}.

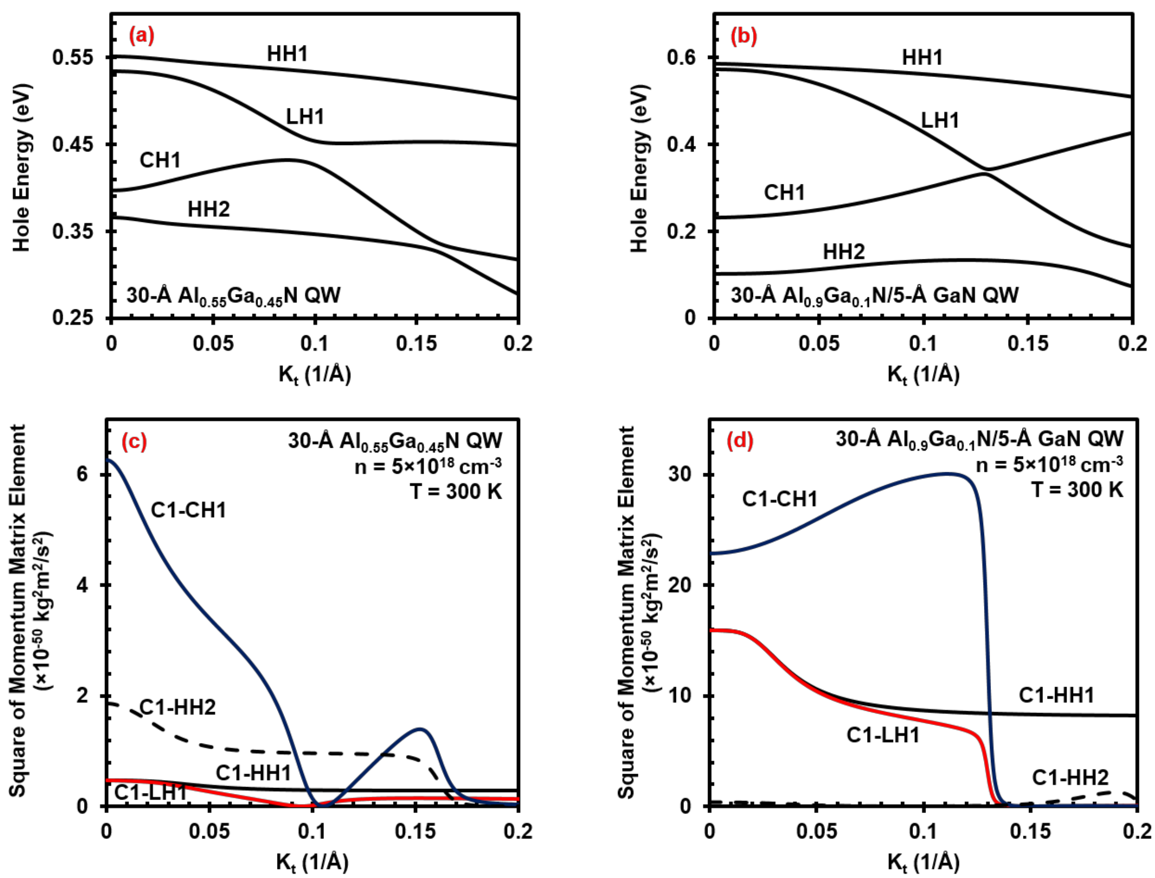

Figure 2. Band edge valence band structures for (a) $Al_{0.55}Ga_{0.45}N$ QW (b) $Al_{0.9}Ga_{0.1}N$-delta-GaN QW and square of momentum matrix element for (c) $Al_{0.55}Ga_{0.45}N$ QW (d) $Al_{0.9}Ga_{0.1}N$-delta-GaN QW. The carrier density is $n = 5\times10^{18}$ cm^{-3}.

To study the light emission properties, spontaneous emission recombination rate per unit volume ($\boldsymbol{R_{sp}}$) for both conventional 3-nm $Al_{0.55}Ga_{0.45}N$ QW and $Al_{0.9}Ga_{0.1}N$-delta-GaN QW are calculated based on the Fermi's Golden rule with considering all the transition between n^{th} conduction band and m^{th} valence subbands. Figure 3 confirms the TE-polarized emission is greater than TM-polarized emission from both QW structures with emission wavelength of ~260 nm, which is caused by the dominant C-HH transition. From the simulation, the total $\boldsymbol{R_{sp}}$ for the $Al_{0.9}Ga_{0.1}N$-delta-GaN QW was calculated to be 30 times larger than that of the conventional 3-nm $Al_{0.55}Ga_{0.45}N$ QW. The significant $\boldsymbol{R_{sp}}$ enhancement by the use of $Al_{0.9}Ga_{0.1}N$-delta-GaN QW is credited to the electron and hole wave function overlap improvement. In addition, previous study mentioned the flexibility of the delta-QW design for deep-UV LEDs by adjusting the delta-GaN QW thickness and the Al-composition in AlGaN sub-QW region. Therefore, this work also calculates another AlGaN-delta-GaN QW structure with 3-Å delta-GaN layer for 260 nm emission, and is compared with conventional AlGaN QWs with different QW thickness at similar emission wavelength. The results show much larger $\boldsymbol{R_{sp}}$ from both delta-QW designs, as compared to conventional AlGaN QWs even with the QW thickness down to 2 nm, which indicates the delta-QW is a promising alternative active region for high-efficiency UV LEDs at 260 nm.

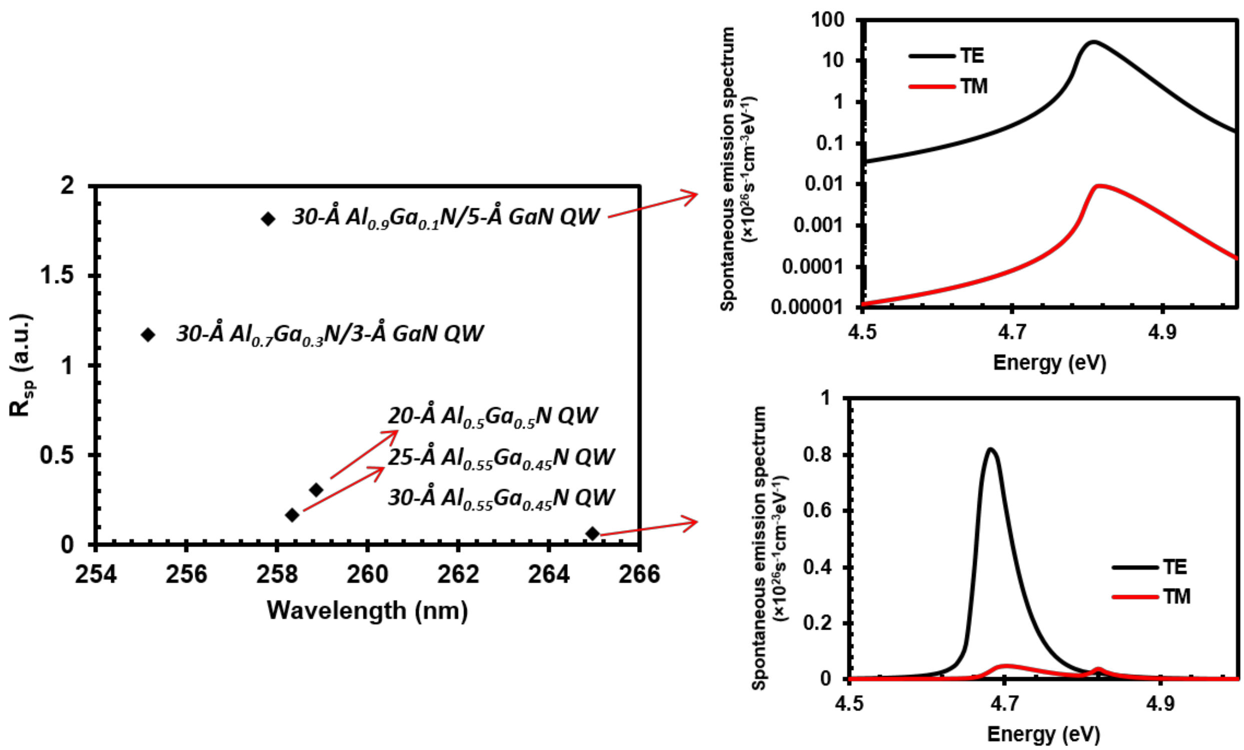

Figure 3. Spontaneous emission recombination rate per unit volume ($\boldsymbol{R_{sp}}$) for 30-Å $Al_{0.9}Ga_{0.1}N$/5-Å GaN QW, 30-Å $Al_{0.7}Ga_{0.3}N$/3-Å GaN QW, and AlGaN QWs with QW thickness of 2 nm, 2.5 nm and 3 nm at room temperature. The carrier density is $n = 5\times10^{18}$ cm^{-3}.

MBE-GROWN ALGAN-DELTA-GAN QUANTUM WELL

To demonstrate the delta-QW for 260 nm emission, a five-period $Al_{0.9}Ga_{0.1}N$-delta-GaN QW was grown by using a Veeco Gen-10 plasma assisted MBE system on AlN/sapphire template with threading dislocation density of 10^{10} cm^{-2}. The sample was loaded into the MBE chamber after a standard solvent cleaning process and outgassed at 200 °C for 7 hours followed by 2 hours at 500 °C. The substrate thermocouple temperature and the RF plasma power were kept at 800 °C and 200 W, respectively, throughout entire epitaxy growth. The 1.65 sccm flow led to a chamber pressure of 1.83×10^{-5} Torr. The growth rate was calibrated to be 5 nm/ min. Figure 4 shows the schematic of the structure with 5 periods of $Al_{0.9}Ga_{0.1}N$-delta-GaN QWs. A 100 nm AlN layer was first grown on the template under a metal rich growth condition to achieve a smooth surface, which is evidenced by a long streaky RHEED pattern shown in figure 4 (a). A 1.5-nm $Al_{0.9}Ga_{0.1}N$ layer was grown before the repeated layers formation. The growth cycle started with a 2-ML GaN, followed by a 1.5-nm $Al_{0.9}Ga_{0.1}N$, a 3-nm AlN and another $Al_{0.9}Ga_{0.1}N$ layer in sequence. Two separate gallium effusion sources were employed to grow 2-ML GaN and $Al_{0.9}Ga_{0.1}N$ separately. The AlN barrier layer was grown by using migration enhanced epitaxy (MEE) to enhance the Al adatom mobility. In addition, two interruptions were added during each cycle growth to desorb the excess Ga on the sample surface. Specifically, the first interruption was employed after the deposition of Al during the AlN MEE growth while the second interruption was used before the 2-ML GaN formation. At the meanwhile, the RF plasma was switched off during the second interruption to avoid the unintentional GaN formation. The heterostructure was capped with a 3-nm AlN layer after the five cycles growth to form the whole 5-period $Al_{0.9}Ga_{0.1}N$-delta-GaN QWs. Figure 4(b) and 4(c) show the RHEED patterns during and after the active region growth, respectively, indicating the smooth surface throughout the entire growth. In addition, an AFM image was taken after the active region growth, which again confirms the active region surface is smooth (RMS = 0.345 nm).

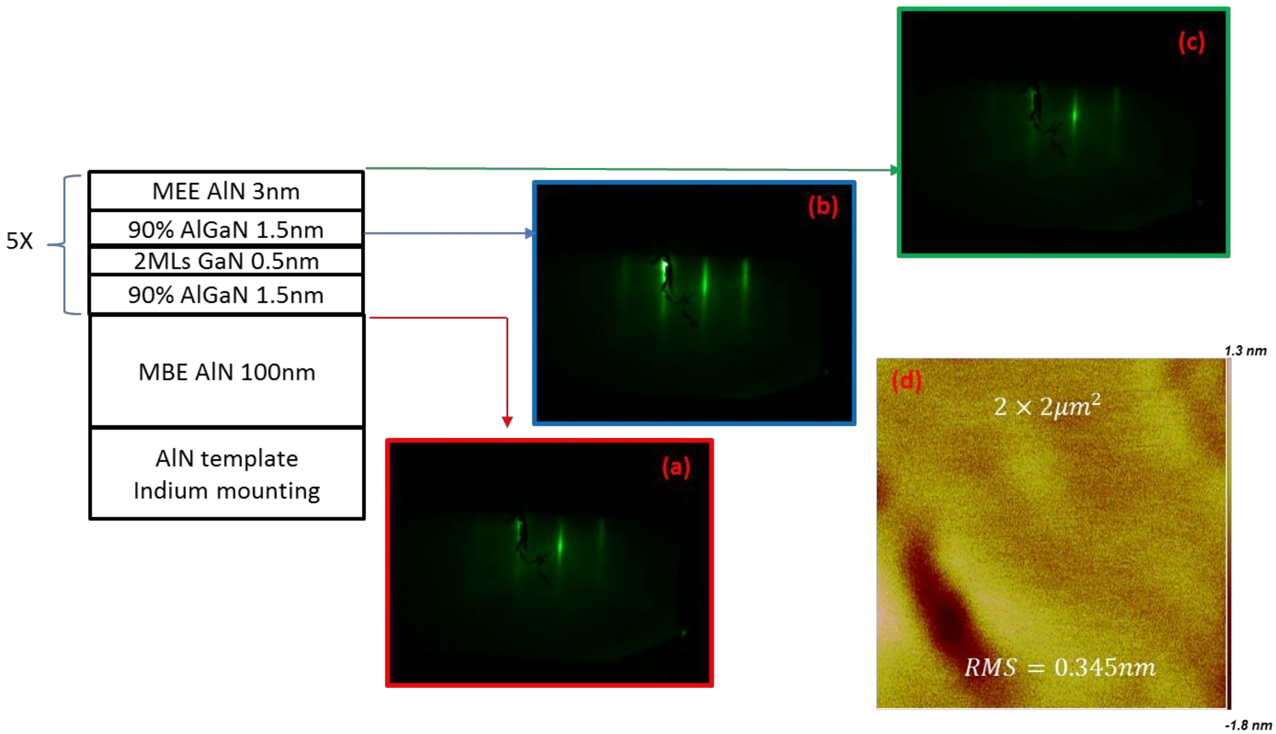

Figure 4. Schematic of the structure with 5 periods of $Al_{0.9}Ga_{0.1}N$-delta-GaN QWs, AFM image of $Al_{0.9}Ga_{0.1}N$-delta-GaN QWs on AlN/sapphire template and RHEED patterns (a) before (b) during (c) after the active region growth. (d) AFM image after the active region growth.

The signature of the $Al_{0.9}Ga_{0.1}N$-delta-GaN heterostructure is directly evidenced from XRD measurements. A 3-nm $Al_{0.9}Ga_{0.1}N$/3-nm AlN heterostructure was also grown with the same condition for comparison. Figure 5 shows high resolution XRD (HR-XRD) ω-2θ scans for 5-period $Al_{0.9}Ga_{0.1}N$-delta-GaN QWs and 5-period $Al_{0.9}Ga_{0.1}N$ QWs. For $Al_{0.9}Ga_{0.1}N$ QWs, there is a shoulder peak near the strong AlN substrate peak, which is corresponding to the 90% AlGaN layer. As a contrast, the XRD spectra for the $Al_{0.9}Ga_{0.1}N$-delta-GaN QW sample showed a strong peak from AlN substrate and secondary peaks from the GaN layers and the measured XRD data was fitted with simulation for 5 periods of 2.05-nm AlN/1.25-nm 90% AlGaN/2-ML GaN/1.25 nm AlGaN, which indicates the successful of the $Al_{0.9}Ga_{0.1}N$-delta-GaN QW growth.

The MBE-grown $Al_{0.9}Ga_{0.1}N$-delta-GaN QW and $Al_{0.9}Ga_{0.1}N$ QWs were also examined by the Z-contrast scanning transmission electron microscope (STEM) too demonstrate the formation of 2-ML GaN. As shown in figure 6 (a) and (b), AlN and $Al_{0.9}Ga_{0.1}N$ layers can be clearly distinguished from both heterostructures based on the Z-contrast. In addition, a thin bright layer is observed in between of the two $Al_{0.9}Ga_{0.1}N$ layers in figure 6 (a) while that is absent in figure 6 (b), which confirms the formation of 2-ML GaN in the MBE-grown $Al_{0.9}Ga_{0.1}N$-delta-GaN QWs. Moreover, an energy-dispersive x-ray spectroscopy scan was performed on the 3-nm $Al_{0.9}Ga_{0.1}N$/3-nm AlN heterostructure, confirming the 90% Al-content from the AlGaN regions. The emission property from the heterostructure was also investigated by a 2-photon PL measurement at room temperature. A strong 259 nm luminescence peak with a full width at half maximum of 12 nm was achieved and shown in figure 6 (c), which is consistent with the simulation results. Therefore, the $Al_{0.9}Ga_{0.1}N$-delta-GaN QW was experimentally demonstrated by the use of plasma assisted MBE system for 260 nm emission.

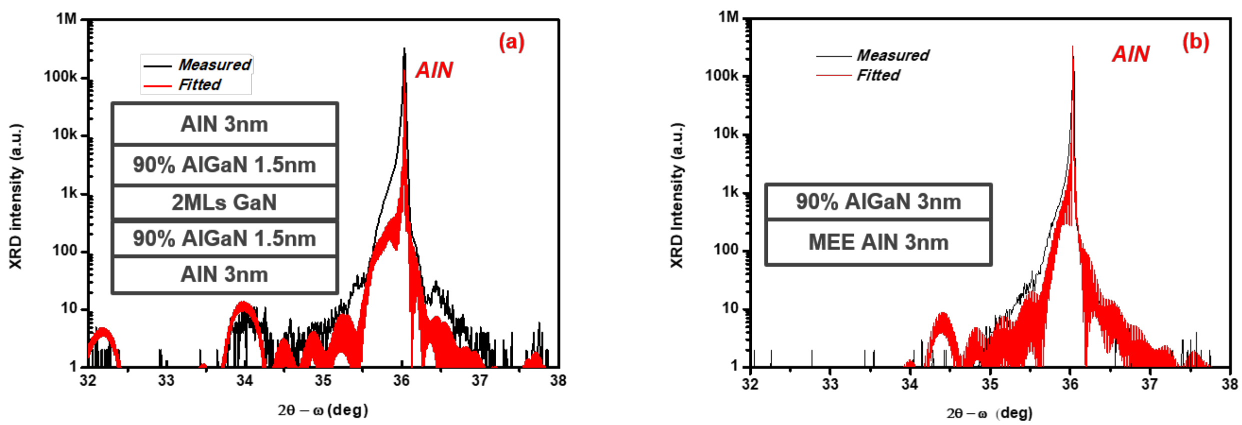

Figure 5. 2θ- ω XRD spectra for (a) 5-period $Al_{0.9}Ga_{0.1}N$-delta-GaN QW and (b) 5-period $Al_{0.9}Ga_{0.1}N$ QW

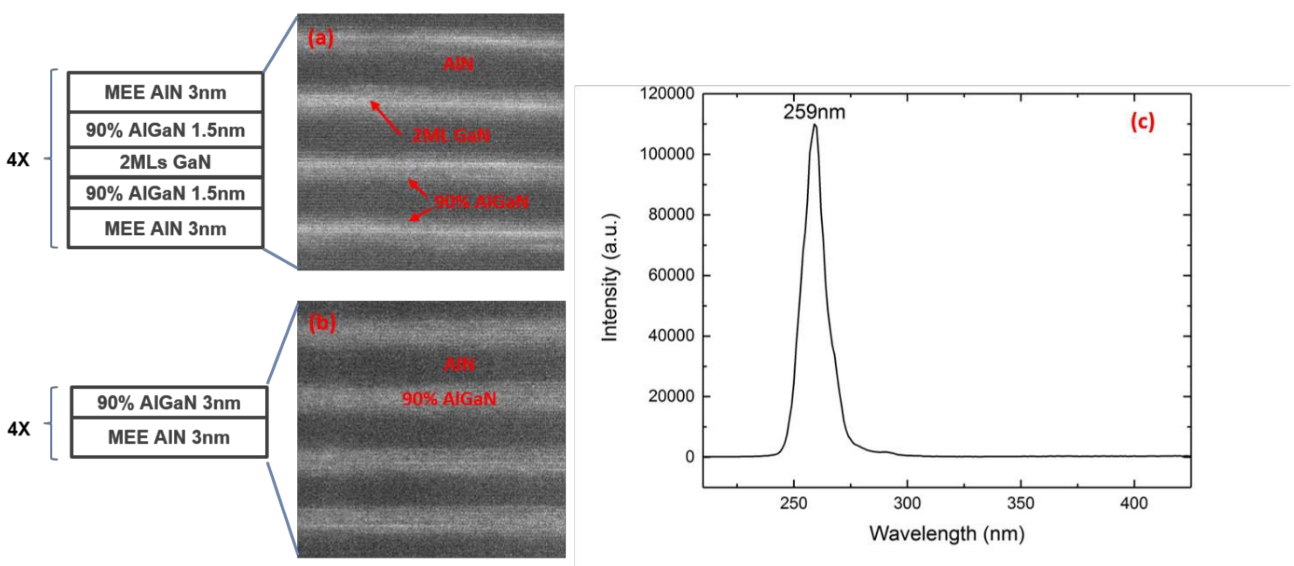

Figure 6. STEM images of (a) $Al_{0.9}Ga_{0.1}N$-delta-GaN QW and (b) 3-nm $Al_{0.9}Ga_{0.1}N$/3-nm AlN heterostructure. Two-photon PL spectrum of $Al_{0.9}Ga_{0.1}N$-delta-GaN QW.

SUMMARY

In conclusion, the delta-QW design offers a potential solution to the problem remained in deep-UV LED active region, such as the quantum confined stark effect. In this study, an $Al_{0.9}Ga_{0.1}N$-delta-GaN QW was designed and investigated for 260 nm emission. The insertion of an ultra-thin delta-GaN layer significantly improves the electron and hole wave function overlap and reduce the QCSE suffered in conventional AlGaN QWs, resulting to a 30 times enhancement in spontaneous emission rate as compared to that of $Al_{0.55}Ga_{0.45}N$ QW at 260 nm. The proposed QW structure was grown by a plasma assisted MBE system and monitored by RHEED. Secondary peaks and bright thin layer were observed by HR-XRD and STEM image, respectively. All these have been hypothesized as signs of 2-ML GaN formation. 2-photon PL measurement shows a strong 260 nm emission from the MBE-grown QW structure, indicating the $Al_{0.9}Ga_{0.1}N$-delta-GaN QW would be a promising alternative active region for deep-UV LEDs.

ACKNOWLEDGMENT

The authors (C. Liu, and J. Zhang) would like to acknowledge the support by the Kate Gleason endowed professorship fund from Rochester Institute of Technology, and by the Office of Naval Research under Award No. N00014-16-1-2524. The authors (K. Lee, S. M. Islam, H. Xing, and D. Jena) would like to thank the support from the University of Notre Dame and the NSF DMREF program (1534303). We would also thank Prof. Sergei Rouvimov from Notre Dame University for technical support with the TEM images and Okan Koksal, Prof. Farhan Rana from Cornell University for two-photon PL measurements.

REFERENCES

[1] Kneissl, M., and Rass, J., [III-Nitride Ultraviolet Emitters: Technology and Applications] Springer Ser. Mater. Sci., Vol. 227 (2016)

[2] Bolton, J. R., Cotton, C. A., [The Ultraviolet Disinfection Handbook], American Water Works Association, Denver (2008)

[3] Vilhunen, S., Särkkä, H., and Sillanpää. M., “Ultraviolet light-emitting diodes in water disinfection,” Environ. Sci. Pollut. Res., 16, 439 (2009)

[4] Muramoto, Y., Kimura, M., and Nouda, S., “Development and future of ultraviolet light-emitting diodes: UV-LED will replace the UV lamp,” Semicond. Sci. Technol. 29, 084004 (2014).

[5] Hirayama, H., Fujikawa, S., Noguchi, N., Norimatsu, J., Takano, T., Tsubaki, K., and Kamata, N., “222-282 nm AlGaN and InAlGaN-based deep-UV LEDs fabricated on high-quality AlN on sapphire,” Phys. Status Solidi A, 206, No. 6, 1176-1182 (2009)

[6] Zhang, Y., Krishnamoorthy, S., Akyol, F., Bajaj, S., Allerman, A. A., Mooseley, M. W., Armstrong, A. M., and Rajan, S., “Tunnel-injected sub-260 nm ultraviolet light emitting diodes,” Appl. Phys. Lett., 110, 201102 (2017).

[7] Jo, M., Maeda, N. and Hirayama, H., “Enhanced light extraction in 260 nm light-emitting diode with a highly transparent p-AlGaN layer,” Appl. Phys. Express, 9, 012102 (2016).

[8] Sun, W., Shatalov, M., Deng, J., Hu, X., Yang, J., Lunev, A., Bilenko, Y., Shur, M., and Gaska, R., “Efficiency droop in 245-247 nm AlGaN light-emitting diodes with continuous wave 2 mW output power,” Appl. Phys. Lett. 96, 061102 (2010).

[9] Kneissl, M., Kolbe, T., Chua, C., Kueller, V., Lobo, N., Stellmach, J., Knauer, A., Rodriguez, H., Einfeldt, S., Yang, Z., Johnson, N. M., and Weyers, M., “Advances in group III-nitride-based deep UV light-emitting diode technology,” Semicond. Sci. Technol. 26, 014036 (2011).

[10] Mehnke, F., Kuhn, C., Stellmach, J., Kolbe, T., Lobo-Ploch, N., Rass, J., Rothe, M. A., Reich, C., Ledentsov, M. Jr., Pristovsek, M., Wernicke, T., and Kneissl, M., “Effect of heterostructure design on carrier injection and emission characteristics of 295 nm light emitting diodes,” J. Appl. Phys., 117, 195704 (2015).

[11] Mehnke, F., Kuhn, C., Guttmann, M., Reich, C., Kolbe, T., Kueller, V., Knauer, A., Lapeyrade, M., Einfeldt S., Rass, J., Wernicke, T., Weyers, M. and Kneissl, M., "Efficient charge carrier injection into sub-250 nm AlGaN multiple quantum well light emitting diodes," Appl. Phys. Lett. 105(5), 051113 (2014).
[12] Zhang, Y., Allerman, A. A., Krishnamoorthy, S., Akyol, F., Moseley, M. W., Armstrong, A. M., and Rajan, S., "Enhanced light extraction in tunnel junction-enabled top emitting UV LEDs," Appl. Phys. Express., 9, 052102 (2016).
[13] Zhang, J., Zhao, H. and Tansu, N., "Effect of crystal-field split-off hole and heavy-hole bands crossover on gain characteristics of high Al-content AlGaN quantum well lasers," Appl. Phys. Lett. 97(11), 111105 (2010).
[14] Zhang, J., Zhao, H. and Tansu, N., "Large optical gain AlGaN-delta-GaN quantum wells laser active regions in mid- and deep-ultraviolet spectral regimes," Appl. Phys. Lett. 98(17), 171111 (2011).
[15] Taniyasu, Y. and Kasu, M., "Polarization property of deep-ultraviolet light emission from C-plane AlN/GaN short-period superlattice," Appl. Phys. Lett., 99, 251112 (2011).
[16] Verma, J., Islam, S. M., Protasenko, V., Kandaswamy, P. K., Xing, H. and Jena, D. "Tunnel-injection quantum dot deep-ultraviolet light-emitting diodes with polarization-induced doping in III-nitride heterostructures," Appl. Phys. Lett., 104, 021105 (2014).
[17] Islam, S. M., Protasenko, V., Rouvimov, S., Xing, H. and Jena, D., "Sub-230 nm deep-UV emission from GaN quantum disks in AlN grown by a modified Stranski-Krastanov mode," Jpn. J. Appl. Phys. 55, 05FF06 (2016).
[18] Verma, J., Kandaswamy, P., Protasenko, V., Verma, A., Xing, H. and Jena, D., "Tunnel-injection GaN quantum dot ultraviolet light-emitting diodes," Appl. Phys. Lett., 102, 041103 (2013).
[19] Liu, C. Ooi, Y. K., Islam, S. M., Verma, J., Xing, H., Jena, D. and Zhang, J., "Physics and polarization characteristics of 298 nm AlN-delta-GaN quantum well ultraviolet light-emitting diodes," Appl. Phys. Lett., 110, 041108 (2017)
[20] Liu, C. Ooi, Y. K., Islam, S. M., Xing, H., Jena, D. and Zhang, J., "234 nm and 246 nm AlN-delta-GaN Quantum Well Deep Ultraviolet Light-Emitting Diodes," Appl. Phys. Lett., 112, 011101 (2018)
[21] Zhao, H., Arif, R. A., Ee, Y. K. and Tansu, N., "Self-consistent analysis of strain-compensated InGaN–AlGaN quantum wells for lasers and light-emitting diodes," IEEE J. Quantum Elect. 45(1), 66-78 (2009).